

# Bidirectional Spiral Pulley Negative Stiffness Mechanism for Passive Energy Balancing

**Jiaying Zhang<sup>1</sup>**

College of Engineering,  
Zienkiewicz Centre for Computational Engineering,  
Swansea University,  
Swansea SA2 8PP, UK  
e-mail: jiaying.zhang@swansea.ac.uk

**Alexander D. Shaw**

College of Engineering,  
Zienkiewicz Centre for Computational Engineering,  
Swansea University,  
Swansea SA2 8PP, UK  
e-mail: a.d.shaw@swansea.ac.uk

**Mohammadreza Amoozgar**

College of Engineering,  
Zienkiewicz Centre for Computational Engineering,  
Swansea University,  
Swansea SA2 8PP, UK  
e-mail: m.amoozgar@swansea.ac.uk

**Michael I. Friswell**

College of Engineering,  
Zienkiewicz Centre for Computational Engineering,  
Swansea University,  
Swansea SA2 8PP, UK  
e-mail: m.i.friswell@swansea.ac.uk

**Benjamin K. S. Woods**

Department of Aerospace Engineering,  
University of Bristol,  
Bristol BS8 1TR, UK  
e-mail: ben.k.s.woods@bristol.ac.uk

*The energy balancing concept seeks to reduce actuation requirements for a morphing structure by strategically locating negative stiffness devices to tailor the required deployment forces and moments. One such device is the spiral pulley negative stiffness mechanism. This uses a cable connected with a pre-tension spring to convert the decreasing spring force into the increasing balanced torque. The kinematics of the spiral pulley is first developed for bidirectional actuation, and its geometry is then optimized by employing an energy conversion efficiency function. The performance of the optimized bidirectional spiral pulley is then evaluated through the net torque, the total required energy, and energy conversion efficiency. Then, an additional test rig tests the bidirectional negative stiffness property and compares the characteristics with the corresponding analytical result. Exploiting the negative stiffness mechanism is of significant interest not only in the field of morphing aircraft but also in many other energy and power reduction applications. [DOI: 10.1115/1.4043818]*

<sup>1</sup>Corresponding author.

Contributed by the Mechanisms and Robotics Committee of ASME for publication in the JOURNAL OF MECHANISMS AND ROBOTICS. Manuscript received October 5, 2018; final manuscript received April 25, 2019; published online July 18, 2019. Assoc. Editor: Andrew P. Murray.

## 1 Introduction

The objective of this paper is to develop an energy balancing system for passive energy balancing. The key component of this objective is using an additional negative stiffness system to balance the positive stiffness of the morphing system, therefore reducing the actuation effort. Although the concept of using negative stiffness systems has been generally used to achieve stiffness changes in a dynamic system [1,2], the alternative use of negative stiffness can be beneficial for statically balanced systems, especially for morphing aircraft. It can be assumed that if the required input, such as force or torque, can be completely eliminated by the negative stiffness system, then in principle no energy is required to move the system other than to overcome dissipation. Therefore, the use of negative stiffness systems is likely to benefit energy-constrained systems, such as those present in the aerospace and automotive industries. Many applications have been proposed that use a negative stiffness for passive energy balancing. An energy balancing adjustment system has been developed for gravity equilibrators, which uses the extended spring to supply or store the necessary energy and the rotation of a fixed geometry bar to produce a statically balanced system [3,4]. A statically balanced compliant mechanism has been proposed by coupling a compliant mechanism with a precompressed plate spring to give a zero stiffness behavior [5]. Some other alternative uses of negative stiffness systems for passive energy balancing have also been investigated, such as for morphing aircraft. A negative stiffness nonlinear overcenter linkage is used on a tilt-rotor blade for active twist. This negative stiffness linkage mechanism uses the stored energy of a compressed spring to rotate the output shaft, resulting in an effectively softened blade that requires a 70% reduction in torque for morphing [6]. Moreover, spring pulley systems have been developed, for instance, a cam-based balancer with a varying radius pulley can preserve moment equilibrium between a constant load and a varying spring length [7,8]. Previous works have been undertaken by Woods et al., where a pneumatic actuator was used to provide kinematic tailoring [9]. The output load line of the actuator was modified to match an assumed torque for driving a compliant morphing aircraft. Then, an extension spring based system was set up to investigate this concept further [10]. The proposed device provides actuation to change the state of the system, such as deforming a structure or lifting a mass; hence, the energy provided by the actuator transforms into an increased potential energy in the system. Once the system returns to its original state, all of the energy provided by the actuator will be recovered, if the system is conservative. It is important to note that the combination of a negative stiffness and a positive stiffness is likely to build a system that can recycle energy; for a conservative system, this recycling will be perfectly efficient. Thus, the negative stiffness device can help to compensate for the required force/torque and energy and therefore use a smaller (and lighter) actuator.

This work extends [6] by considering the application to a specific design target taken from a relevant morphing structure application, which is different from the previous work on the concept that looked only at balancing a fixed direction. Although the negative stiffness system can only help to produce a passive energy balancing system, unidirectivity is the drawback in the pulley system, which will restrict further applications such as bidirectional actuation requirements. Therefore, a bidirectional spiral pulley negative stiffness (BSPNS) concept is proposed, which is capable of generating the satisfactory bidirectional torque versus rotation profile. The energy used in an actuator is usually nonrecoverable, but the BSPNS device can provide energy to actuate and then be back-drivable by the elastic load in the system. Recently, a mechanism has been proposed that implements a linkage with springs to produce the bidirectional negative stiffness [11]. While the same passive energy balancing effect can be produced, the spiral pulley negative stiffness device is constructed from simpler elements and is more suitable for large load requirements.

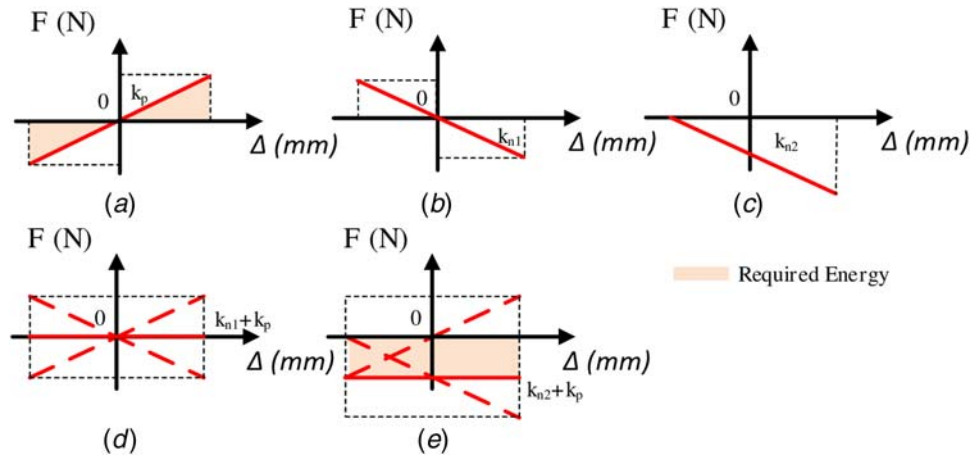


**Fig. 1 Schematic of the integrated bidirectional system force curve.  $k_p$  is the stiffness of the load system and  $k_{n1}$  and  $k_{n2}$  are the negative stiffness systems. (a) Bidirectional increasing force system, (b) bidirectional decreasing force system, (c) unidirectional decreasing force system, (d) integrated system of (a) and a bidirectional negative stiffness system, and (e) integrated system of (a) and a unidirectional negative stiffness system.**

This paper is organized into two parts. In the first part, BSPNS mechanism is investigated by extending the proposed wrapping cam system. The kinematics is modified to adapt to the bidirectional drive line of the negative stiffness mechanism from the previous work [6]. Two extension springs are connected with a constant radius pulley to produce a bidirectional required torque, and the geometry of the bidirectional spiral pulley was optimized for the design case. In the second part, an experimental demonstrator was built and tested, confirming the ability of the bidirectional spiral pulley negative stiffness concept to actuate a representative load.

## 2 Bidirectional Spiral Pulley Negative Stiffness Mechanism

Although the previous negative stiffness devices can provide a satisfactory result for passive energy balancing, the motion of the mechanism is fixed to be opposite to the wrap direction, and this unidirectivity will restrict further bidirectional applications [6,10]. Figure 1 shows a schematic of the integrated system force curve by coupling two kinds of negative stiffness system. Many energy-required systems have a bidirectional elastic force response as shown in Fig. 1(a), where the required force increases with the larger stroke to overcome the elastic deformation in both directions. Such a system is a positive stiffness system from the initial condition for both actuation directions. Although previous works [6,10] have shown that negative stiffness can be used to produce static balancing for such a system to give a zero stiffness property, different negative stiffness systems have different characteristics, which can be seen in Figs. 1(b) and 1(c). Figure 1(b) shows a bidirectional negative stiffness, which is distinct from the unidirectional negative stiffness shown in Fig. 1(c), and a bidirectional negative stiffness system is more suited to passive energy balancing of a bidirectional positive stiffness system. In order to illustrate the concept visually, Figs. 1(d) and 1(e) show the positive system in Fig. 1(a) coupled with the negative stiffness systems shown in Figs. 1(b) and 1(c), respectively. Both negative stiffness systems can produce an energy balancing system where the actuation is zero (i.e., a constant force), but the results are different from the viewpoint of energy. The integrated system by coupling a unidirectional negative stiffness system still requires energy for actuation no matter how the two curves shown in Fig. 1(e) are adjusted. Therefore, the bidirectional negative stiffness reveals better performance and should be investigated for passive energy balancing of mechanical systems to reduce the actuation requirements and improve the energy efficiency.

Therefore, an innovative concept for designing a BSPNS mechanism is proposed, which can be more beneficial than fixed directional negative stiffness devices. Figure 2 shows a full scheme of the bidirectional spiral pulley with a constant radius output pulley. The bidirectional spiral pulley is a combination of two spiral pulleys mounted onto a central shaft and supported by two bearings. It is worth mentioning that the BSPNS unit can provide a bidirectional motion by rotating the shaft clockwise (B) or anticlockwise (A), as shown in Fig. 2. This bidirectional feature provides a better solution for many practical applications than single-directional devices.

## 3 Kinematics Analysis

The complicated kinematics of one spiral pulley and spooling cable is first investigated, as shown in Fig. 3. Although any profile of the pulley can be used to produce the variation in radius, an exponential radius function was chosen as potentially the best match to the desired nonlinear force profile. The detailed geometry definition of the spiral pulley is shown in Fig. 3. The spiral pulley is first defined as an exponential radius profile in polar coordinates about the center of rotation  $O$

$$r = r_0 + k_1 e^{k_2(\theta + \delta_0)} \quad (1)$$

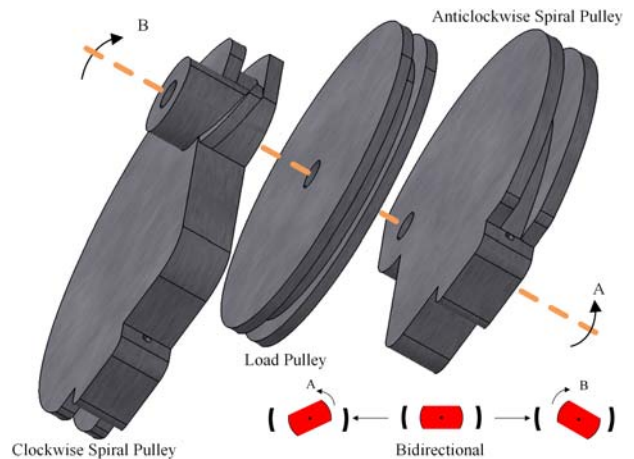


**Fig. 2 Schematic diagram of the proposed bidirectional spiral pulley**

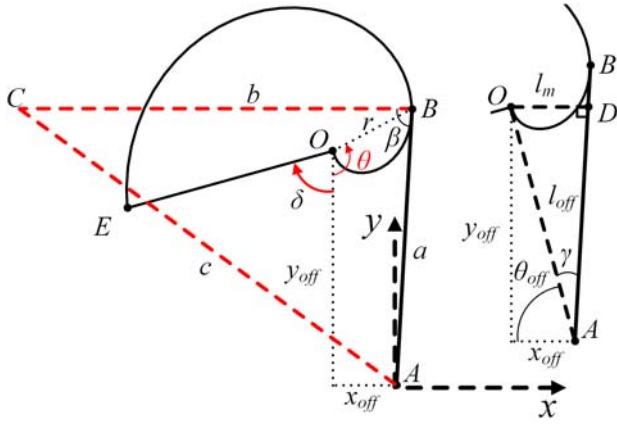


**Fig. 3** Spiral pulley geometry analysis with moment arm details

where  $\delta$  is spiral pulley rotation angle and  $\theta$  is a parameter associated with it;  $\delta_0$  is initial pulley rotation angle; and  $r_0$ ,  $k_1$ , and  $k_2$  are parameters of the spiral profile, respectively. A wide range of different radius profiles can be used for the spiral pulley, with different shape functions being better suited to different load profiles. The exponential function used here has been shown to be well suited to the linear stiffness we wish to balance in this case [6,10].

Figure 3 shows that the cable is wrapped around the spiral pulley and point B is the initial point of contact. The Cartesian coordinates can then be defined with the origin point at A, and the coordinates of any point B can then be defined as follows:

$$x_B = x_{off} - r \sin \theta \quad (2)$$

$$y_B = y_{off} - r \cos \theta \quad (3)$$

Therefore, the length of the vector  $\overline{AO}$  is equal to

$$l_{off} = \sqrt{x_{off}^2 + y_{off}^2} \quad (4)$$

In addition, length of the cable  $a$  between the origin point A and point B is equal to

$$a = \sqrt{x_B^2 + y_B^2} \quad (5)$$

As mentioned above, the cable is wrapped around the spiral pulley from point B to the cable anchor point E. The arc length of the wrapped cable is then obtained as follows:

$$\begin{aligned} S &= \int_{\theta(B)}^{\theta(E)} \sqrt{r^2 + \left(\frac{dr}{d\theta}\right)^2} d\theta \\ &= \int_{\theta(B)}^{\theta(E)} \sqrt{(r_0 + k_1 e^{k_2(\theta+\delta)})^2 + (k_2 k_1 e^{k_2(\theta+\delta)})^2} d\theta \end{aligned} \quad (6)$$

Therefore, the total length of the cable from point A to point E is equal to

$$L = b + S \quad (7)$$

Since the length of the cable between spiral pulley and extension spring is essentially constant, the rotation of the spiral pulley leads to the release of a portion of the cable. The change in the spring length can be calculated by subtracting the total cable length evaluated at each spiral pulley rotation angle  $\delta$ , from the total cable length at the initial pulley rotation angle  $\delta_0$ .

$$\Delta L = L_\delta - L_{\delta_0} \quad (8)$$

Then, the moment produced by the force in the cable varies due to the change of the moment arm  $\overline{OD}$ , which is defined as  $l_m$ , the length of the vector perpendicular to the straight cable  $\overline{AB}$ . In

order to calculate the length  $l_m$ , it is necessary to add an additional guide  $\overline{BC}$  with an arbitrary fixed length of  $\overline{BC} = b$  and parallel to the horizontal axis. The coordinates of point C can then be determined as follows:

$$x_C = x_B - b \quad (9)$$

$$y_C = y_B \quad (10)$$

$b$  is taken to be 50 mm (can be arbitrary value) for analysis here. The length  $c$  of vector  $\overline{AC}$  is equal to

$$c = \sqrt{x_C^2 + y_C^2} \quad (11)$$

The angle  $\beta$  can be obtained by using the law of cosines with the known  $a$ ,  $b$ , and  $c$ , which is

$$\beta = \cos^{-1} \left[ \frac{a^2 + b^2 - c^2}{2ab} \right] \quad (12)$$

The angle of the pulley rotation point relative to the origin  $\theta_{off}$  is

$$\theta_{off} = \tan^{-1} \left( \frac{y_{off}}{x_{off}} \right) \quad (13)$$

The moment arm angle  $\gamma$  in Fig. 3 can therefore be derived by given  $\beta$  and  $\theta_{off}$

$$\gamma = \pi - \beta - \theta_{off} \quad (14)$$

The length  $l_m$  of the moment arm  $\overline{OD}$  can finally be solved by Eqs. (4) and (14)

$$l_m = l_{off} \sin \gamma = \sqrt{x_{off}^2 + y_{off}^2} \sin \gamma \quad (15)$$

It is obvious that the above analysis is derived for any point B on the profile of the spiral pulley. Therefore, in order to match the practical situation, it is important to confirm the unique position of point B for each rotation angle  $\delta$ . In other words, extra conditions should be considered to find the point of tangency between the straight portion of the cable  $\overline{AB}$  and the spiral pulley surface. From the viewpoint of the geometry shown in Fig. 3, the point of tangency occurs when point B has the minimum corresponding angle  $\beta$ . Meanwhile, the value of angle  $\gamma$  could be considered as a function of variable  $\theta$ , and the minimum corresponding angle  $\gamma$  can therefore be solved by differentiating Eq. (12) with respect to  $\theta$  and setting the result equal to 0. Thus,

$$\left. \frac{d\beta}{d\theta} \right|_{\min \beta} = 0 \quad (16)$$

The spring is designed as an energy storage device with an initial length  $L_0$  as mentioned above. The force  $F_s$  in the spring at the current position can therefore be obtained as follows:

$$F_s = K(L_0 - \Delta L) \quad (17)$$

where  $K$  is the spring constant, and the initial tension that exists in practical tension springs will be further discussed. Finally, the torque produced by the spiral pulley can be then obtained from Eqs. (8) and (15) for each rotation angle  $\delta$ , as follows:

$$T_s = F_s l_m \quad (18)$$

Therefore, as the spiral pulley rotates, its effective diameter changes, and the moment arm produced by the profile of the spiral pulley varies. This effect can be tailored to give negative stiffness and optimized for a given actuation role. Then, the kinematics is modified to adapt to the bidirectional drive line of the negative stiffness mechanism. Figure 4 shows that the cable is wrapped around the spiral pulley and the radius of the spiral pulley at the center of rotation is  $r$ . Since the motion of the mechanism should be opposite to the wrap direction, the radius of the spiral pulley

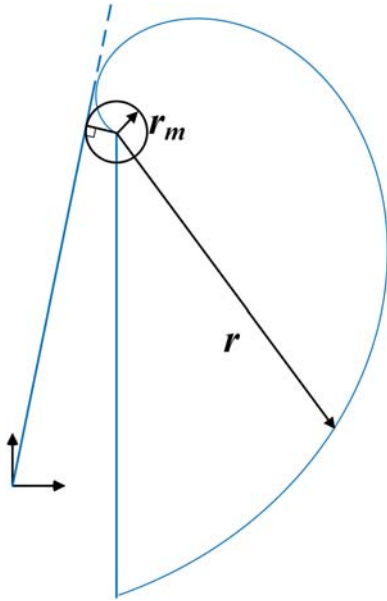


**Fig. 4 Updated spiral pulley geometry details**

should become infinitesimal that is impossible in practical application. Therefore, a small constant radius pulley is attached to the spiral pulley, and the radius should be calculated based on the spiral pulley geometry to avoid a snap and is given by

$$r_m = r_0 + k_1 e^{k_2(\theta + \delta + \delta_0)} = r_0 + k_1 e^{k_2(\theta + \delta_0)} \quad (19)$$

where  $\delta = 0$ . This implies that the wrapped cable is tangent to both the spiral pulley and the attached constant radius pulley, which means that the torque will be changed smoothly, as shown in Fig. 4.

Therefore, the rotation of the bidirectional spiral pulley through 0 deg leads to the release of the cable from one spiral pulley and wraps the cable of the other spiral pulley. For example, if the rotation is clockwise, the clockwise spiral pulley will release a portion of the cable and the anticlockwise spiral pulley will wrap a portion of the cable (vice versa). The torque produced by the clockwise rotation bidirectional spiral pulley can then be obtained from Eqs. (18) and (19) for each rotation angle  $\delta$ , as follows:

$$T_b = F_{s1}l_{m1} - F_{s2}l_{m2} = F_{s1}l_{m1} - F_{s2}r_m \quad (20)$$

The forces  $F_{s1}$  and  $F_{s2}$  in the springs relate to the clockwise spiral pulley and the anticlockwise spiral pulley, respectively.  $l_{m1}$  is the moment arm of the clockwise spiral pulley, which can be obtained by Eq. (15).  $l_{m2}$  is the moment arm of the anticlockwise spiral pulley, which is equal to  $r_m$  in the case of clockwise rotation. Notably, it can be seen that  $r_m$  is the smallest radius in Eq. (19), so that an increasing total torque could be produced.

Finally, in order to optimize the performance of the energy balancing system, an objective energy conversion efficiency function is proposed to make the torque provided by the spiral pulley system match the required torque as closely as possible. To accomplish this, an energy conversion efficiency metric is defined as follows:

$$\eta_{ef} = \frac{E_0}{E_r} \quad (21)$$

where  $E_0$  is the output energy provided from the bidirectional spiral pulley negative stiffness mechanism,

$$E_0 = \int_0^{\delta_f} |T_b| d\delta \quad (22)$$

and  $E_r$  is the required energy to actuate the positive stiffness of the morphing system.

$$E_r = \int_0^{\delta_f} |T_f| d\delta \quad (23)$$

where  $T_f$  is the required torque for each rotation angle  $\delta$ . Then, an energy conversion efficiency-based objective function is proposed, and the nonlinear programming solver *fmincon* is used to optimize the objective function.

## 4 Design Case

In order to show the efficacy of the bidirectional spiral pulley negative stiffness mechanism for energy balancing, a particular design scenario is considered. Two linear extension springs are used as the bidirectional load for the positive stiffness of the morphing system, which represents the energy required to be balanced by the bidirectional negative stiffness mechanism. The output rotation range was prescribed as  $-150 \text{ deg} \leq \delta \leq 150 \text{ deg}$  to show the ability of this bidirectional passive energy balancing concept. A target load torsional stiffness of 0.0074 Nm/deg was chosen, and a commercially available spring was found with a measured spring constant of  $K_l = 88 \text{ N/m}$  (Ashfield Spring Ltd; part number S.30) by connecting four springs in series. Since the spring is always extended and the spring will be still extended after actuation, the initial tension in the commercial tension springs can be neglected. The geometric parameters of the spiral pulley were optimized using the nonlinear programming solver *fmincon* in the MATLAB's Global Optimization Toolbox. The objective function is the energy conversion efficiency function proposed in Eq. (21), and the optimized parameters are listed in Table 1. The bidirectional spiral pulley shape is shown in Fig. 5 along with the constant 13 mm radius load pulley. Meanwhile, the schematic of the design case for energy balancing by using the bidirectional spiral pulley negative stiffness mechanism is also shown in Fig. 5.

With the optimized parameters obtained above, the performance predicted for this bidirectional spiral pulley geometry shows a good match with the bidirectional torque requirements. Figure 6 shows that the evolution of torque with rotation for the BSPNS mechanism and the load springs and the net torque of the whole system. The torque provided by the two spiral pulleys of the BSPNS mechanism matches the torque required closely, including overcoming the opposite required torque  $F_{s2}r_m$ .

Integrating the torque versus rotation curves provides the mechanical energy required to drive the load, as shown in Fig. 7. Comparing the energy required with and without the negative stiffness mechanism shows that the BSPNS mechanism has a strong ability to passively balance the required torque. Figure 7 shows that the predicted energy reduction is almost 96%, with the energy required reduced from 0.025 J to 0.001 J. The BSPNS mechanism is therefore predicted to be able to store and passively transfer 0.024 J of energy.

**Table 1 Optimized parameters for bidirectional spiral pulley**

Parameter	Lower bound	Upper bound	Optimized value	Units
Initial radius, $r_0$	-30/1000	10/1000	-0.0083	m
Pre-exponent term, $k_1$	-0.001	0.020	0.0051	—
Exponent term, $k_2$	0	1	0.3701	—
Initial pulley rotation angle $\delta_0$	$-50 \cdot \pi / 180$	$50 \cdot \pi / 180$	0.5054	rad
Drive spring extension, $L_0$	-0.05	0.4	0.2	m
Drive spring rate, $K$	100	1400	69/4	N/m
$x_{off}$	-0.1	0.1	0.0140	m
$y_{off}$	-0.05	0.10	0.0417	m

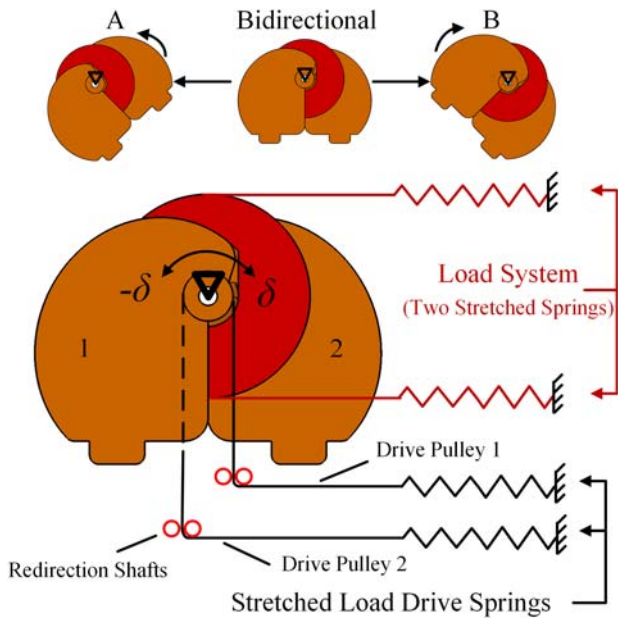


**Fig. 5 Schematic of the bidirectional spiral pulley negative stiffness mechanism for energy balancing**

The energy conversion efficiency objective curve plotted in Fig. 8 shows that the optimized configuration of the bidirectional torque shaft provides significant benefits in terms of energy efficiency. Moreover, it also shows that the bigger the angle of rotation, the less the initial energy lost.

A test rig was built to allow for the experiment testing and validation of the BSPNS concept. The test rig was built on aluminum rails, and labeled top and internal views of the completed test rig are shown in Fig. 9. The bidirectional pulley and box frame were three-dimensional (3D) printed. The pulley was mounted onto a central shaft, which was supported by bearings set into the box mounted to the frame, as can be seen clearly in Fig. 9. Two shafts with bearings were used as redirection pulleys, and the offsets between the pulley rotation point and the redirection pulleys for the drive spring  $x_{off}$  and  $y_{off}$  are shown in Table 1 and provide sufficient clearance for the pulley. The fixed ends of the springs were mounted to tight brackets on the frame, and high-strength spectra cordage was wrapped around the corresponding pulley and connected to each spring. The assembled test rig was then measured using a Zwick load test machine to provide output

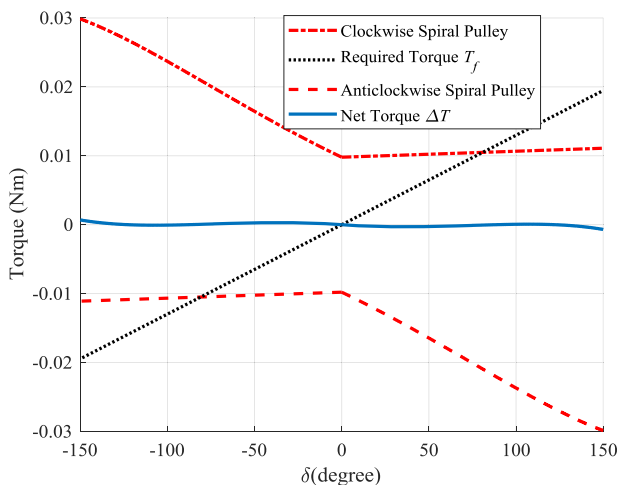


**Fig. 6 Predicted torque with the optimized bidirectional spiral pulley**

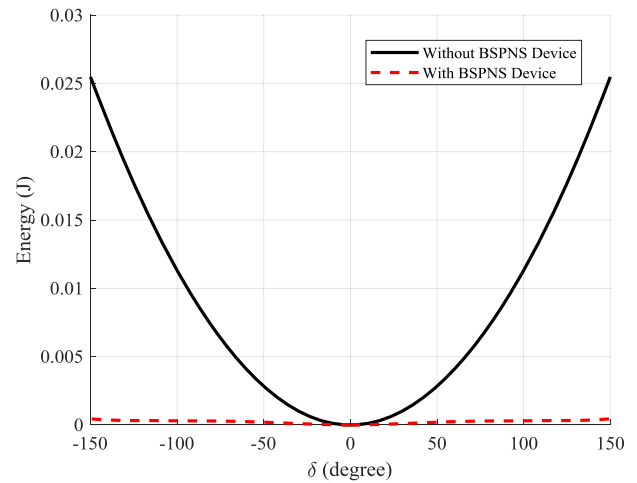


**Fig. 7 Comparison of the predicted energy required with and without BSPNS mechanism**

force. One high-strength spectra cordage is connected to the regular pulley and the test machine to substitute the corresponding spring, and other springs are retained, as shown in Fig. 9. The initial angle of the spiral pulley is  $-157$  deg. The experimentally measured force is compared with the predicted required torque  $T_f$  from the analysis shown in Fig. 6.

Figure 10 shows the experimentally measured and analytically predicted evolution of the force for the device. The torque is minimum ( $-0.008$  Nm) in the initial state, and the torque increases with increasing displacement until the maximum ( $0.008$  Nm) is obtained. The discrepancy between the experimental result and the analytical result is because of friction. The friction of the device is neglected in the predictions, and the angle is measured by dividing the measured displacement by the known radius of the regular pulley. The trend of the torque requirement system is satisfied between the experimental and the analytical results, and the results show that the spiral pulley negative stiffness device allows for a drastic reduction in the actuation requirement.

Once assembled, the test rig was tested for passive energy balancing in each rotation configuration. Because the net torque of the integrated system is nearly zero and hard to test, the different rotation configurations are shown here to imply the neutral stability of the system. The red label in Fig. 11 corresponds to the black mark shown in Fig. 9, which shows the configuration of the load pulley. Figure 11(a) shows selected configurations in the anticlockwise

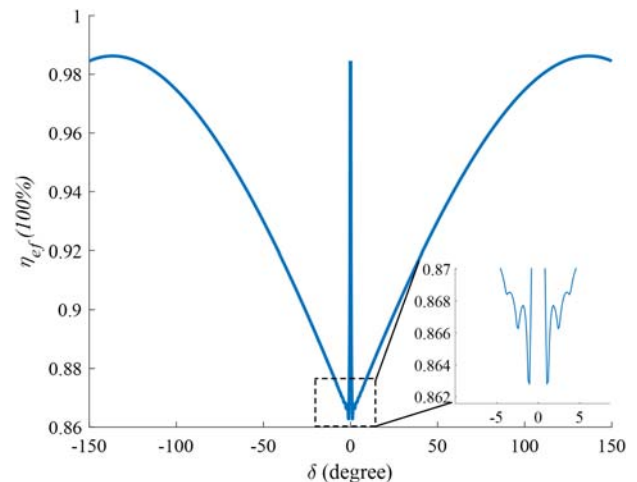


**Fig. 8 Evolution of efficiency with bidirectional rotation**

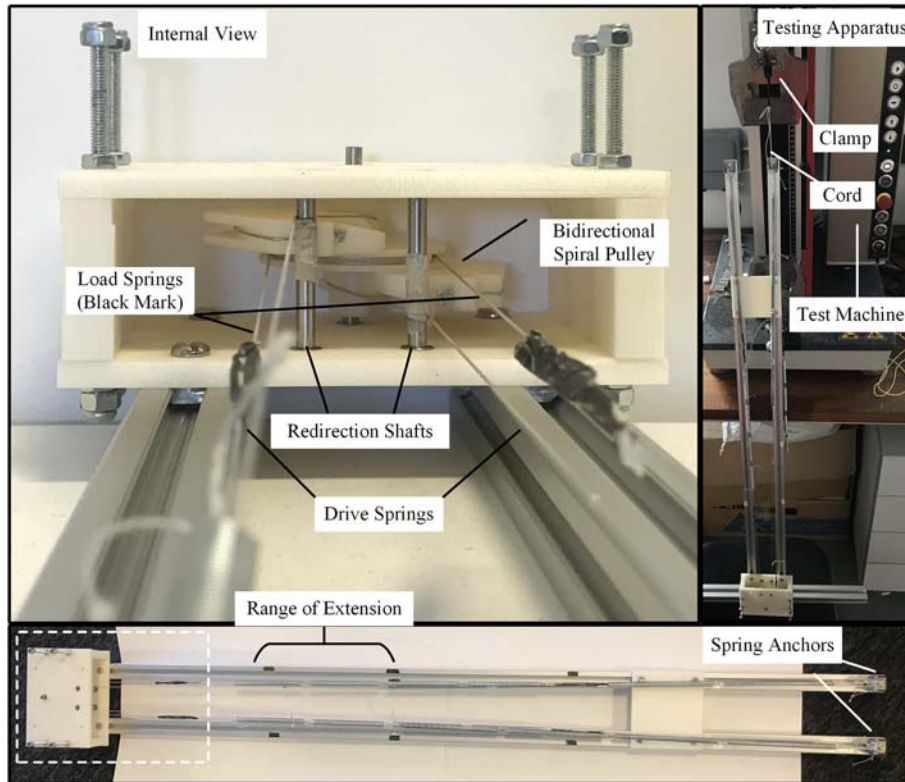


Fig. 9 BSPNS mechanism test rig

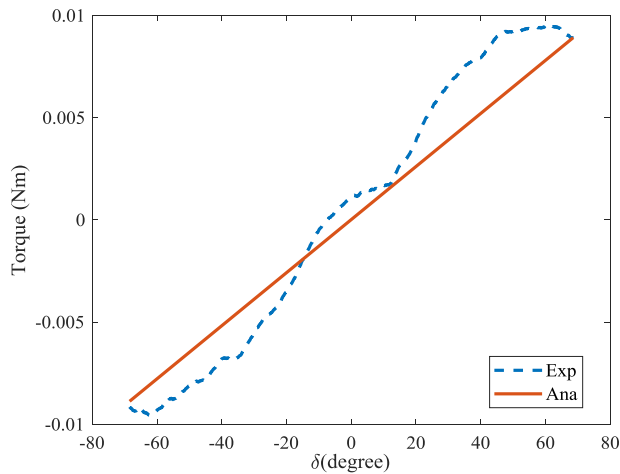


Fig. 10 Comparison of experimental and analytical required torque  $T_r$  for the BSPNS mechanism

rotation, while Fig. 11(b) shows selected configurations in the clockwise rotation. It is worth noting that this test rig can stay in any configuration in both rotation directions as it is a passive energy balancing system, and only selected configurations are shown here.

Based on this investigation, the bidirectional spiral pulley negative stiffness can provide a significant contribution to balance a positive stiffness system. In some practical applications, the external disturbance, such as the aerodynamic load or hysteresis behavior of the structure, will influence the negative stiffness mechanism to eliminate the required force or moment completely. But high energy conversion efficiency can be optimized, which allows most of the required energy to be balanced by using the bidirectional spiral pulley negative stiffness mechanism, and a small actuator could be used to compensate for the difference between these two systems. The work presented here is intended to show the energy balancing concept and the tailorability to different positive stiffness systems. Although the improvement provided by the spiral pulley negative stiffness mechanism is shown for a specific load case, there are potentially a wide range of applications, including different actuators and many different load profiles to be driven.

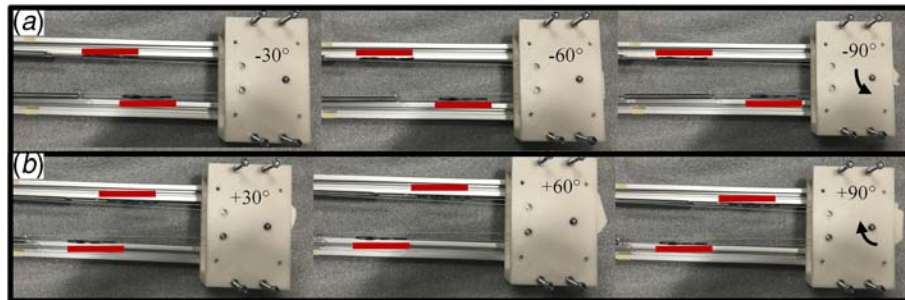


Fig. 11 Selected configurations of the BSPNS mechanism for passive energy balancing (Color version online.)

## 5 Conclusion

A new concept for using a bidirectional spiral pulley negative stiffness mechanism for passive energy balancing has been presented. A spiral pulley negative stiffness mechanism was first proposed as the negative stiffness system by using a pre-tensioned spring. The kinematics of the spiral pulley was introduced and then extended to bidirectionality to satisfy a bidirectional actuation requirement. An energy conversion efficiency function was introduced to provide a basis for evaluation and also act as the objective function to optimize the geometry of the spiral pulley simultaneously. The optimized spiral pulleys were shown to be able to generate torque that matches the required torque of the bidirectional required torque closely. Thus, a significant contribution can be provided by the negative stiffness mechanism to balance the positive stiffness system. Experimental results proved the ability of the bidirectional spiral pulley negative stiffness device to reduce the actuation load by applying the pre-stored energy. While the example used in this paper is relatively simple, it provides insight into the low energy actuation design problem, both in the field of morphing aircraft and in other fields.

The demonstrator of bidirectional spiral pulley negative stiffness mechanism is shown here.<sup>2</sup> Figure 11 shows selected configurations from this video.

## Acknowledgment

This research leading to these results has received funding from the European Commission under the European Union's Horizon 2020 Framework Programme "Shape Adaptive Blades for Rotor-

craft Efficiency" (Grant No. 723491; Funder ID: 10.13039/5011000 00780).

## References

- [1] Karnopp, D., 1995, "Active and Semi-Active Vibration Isolation," *ASME J. Mech. Des.*, **117**(B), pp. 177–185.
- [2] Churchill, C. B., Shahan, D. W., Smith, S. P., Keefe, A. C., and McKnight, G. P., 2016, "Dynamically Variable Negative Stiffness Structures," *Sci. Adv.*, **2**(2), pp. e1500778–e1500778.
- [3] Chu, Y.-L., and Kuo, C.-H., 2017, "A Single-Degree-of-Freedom Self-Regulated Gravity Balancer for Adjustable Payload," *ASME J. Mech. Robot.*, **9**(2), p. 021006.
- [4] Barents, R., Schenk, M., van Dorsser, W. D., Wisse, B. M., and Herder, J. L., 2011, "Spring-to-Spring Balancing as Energy-Free Adjustment Method in Gravity Equilibrators," *ASME J. Mech. Des.*, **133**(6), p. 061010.
- [5] Hoetmer, K., Herder, J. L., and Kim, C. J., 2009, "A Building Block Approach for the Design of Statically Balanced Compliant Mechanisms," ASME 2009 International Design Engineering Technical Conferences and Computers and Information in Engineering Conference, San Diego, CA, Aug. 30–Sept. 2, pp. 313–323.
- [6] Zhang, J., Shaw, A. D., Mohammadreza, A., Friswell, M. I., and Woods, B. K. S., 2018, "Spiral Pulley Negative Stiffness Mechanism for Morphing Aircraft Actuation," ASME 2018 International Design Engineering Technical Conferences and Computers and Information in Engineering Conference, Quebec, Canada, Aug. 26–29, p. V05BT07A003.
- [7] Schenk, M., and Guest, S. D., 2014, "On Zero Stiffness," *Proc. Inst. Mech. Eng. Part C J. Mech. Eng. Sci.*, **228**(10), 1701–1714.
- [8] Ostler, J., and Zwick, K., 1939, "Power Equalizing Device," U.S. Patent No. 2,178,122.
- [9] Woods, B. K. S., Friswell, M. I., and Wereley, N. M., 2014, "Advanced Kinematic Tailoring for Morphing Aircraft Actuation," *AIAA J.*, **52**(4), pp. 788–798.
- [10] Woods, B. K., and Friswell, M. I., 2016, "Spiral Pulley Negative Stiffness Mechanism for Passive Energy Balancing," *J. Intell. Mater. Syst. Struct.*, **27**(12), pp. 1673–1686.
- [11] Zhang, J., Shaw, A. D., Amoozgar, M., Friswell, M. I., and Woods, B. K. S., 2019, "Bidirectional Torsional Negative Stiffness Mechanism for Energy Balancing Systems," *Mech. Mach. Theory*, **131**(2019), pp. 91–107.

<sup>2</sup><https://www.youtube.com/watch?v=JW-WkWRUqno>